ACS OMEGA

Open Access

http://pubs.acs.org/journal/acsodf

Article

Radical Scavenging, Hemocompatibility, and Antibacterial Activity against MDR *Acinetobacter baumannii* in Alginate-Based Aerogels Containing Lipoic Acid-Capped Silver Nanoparticles

Kevin D. Martínez-García, Tonatzin Zertuche-Arias, Johanna Bernáldez-Sarabia, Enrique Iñiguez, Thomas Kretzchmar, Tanya Amanda Camacho-Villegas, Pavel H. Lugo-Fabres, Alexei F. Licea Navarro, Jorge Bravo-Madrigal,* and Ana B. Castro-Ceseña*

Cite This: *ACS Omega* 2024, 9, 2350−2361

Read Online

ACCESS | Metrics & More | Article Recommendations

ABSTRACT: Retaining the hemocompatibility, supporting cell growth, and exhibiting anti-inflammatory and antioxidant properties, while having antimicrobial activity, particularly against multidrug-resistant bacteria (MDR), remain a challenge when designing aerogels for biomedical applications. Here, we report that our synthesized alginate-based aerogels containing either 7.5 or 11.25 μg of lipoic acid-capped silver nanoparticles (AgNPs) showed improved hemocompatibility properties while retaining their antimicrobial effect against MDR *Acinetobacter baumannii* and the reference strain *Escherichia coli*, relative to a commercial dressing and polymyxin B, used as a reference. The differences in terms of the microstructure and nature of the silver, used as the bioactive agent, between our synthesized aerogels and the commercial dressing used as a reference allowed us to improve several biological properties in our aerogels with respect to the reference commercial material. Our aerogels showed significantly higher antioxidant capacity, in terms of nmol of Trolox equivalent antioxidant capacity per mg of aerogel, than the commercial dressing. All our synthesized aerogels showed anti-inflammatory activity, expressed as nmol of indomethacin equivalent anti-inflammatory activity per mg of aerogel, while this property was not found in the commercial dressing material. Finally, our aerogels were highly hemocompatible (less than 1% hemolysis ratio); however, the commercial material showed a 20% hemolysis rate. Therefore, our alginate-based aerogels with lipoic acid-capped AgNPs hold promise for biomedical applications.

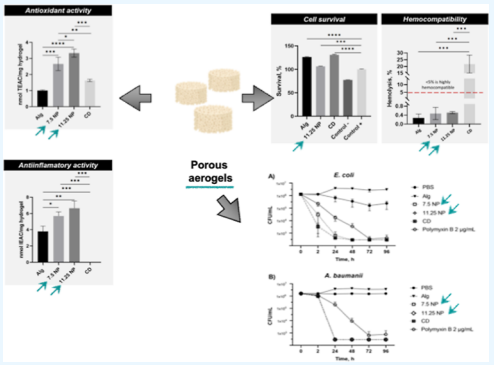

1. INTRODUCTION

Aerogels are used as wound dressings and delivery systems for antibacterial agents[1−3] and are used regularly to reduce wound exposure to the environment to prevent bacterial infection, compress the wound, and stop bleeding. However, available topical products are not always indicated or suitable for all patients, especially those with comorbidities such as cancer, diabetes, hypertension, or vascular disease.[4,5] Furthermore, among the many aerogels options, from simple materials such as nonadherent dressings to modern options such as foam, hydrocolloid, alginate, or negative pressure aerogels, gauze remains one of the most widely used materials for traditional wound care.[5,6] However, the use of conventional gauze as a dressing for second-intention healing of postsurgical wounds tends to cause more pain than other types of occlusive dressings since it involves frequent dressing changes.[7] Additionally, limited results from controlled clinical trials suggest a lack of effectiveness concerning evidence.[5,8] Therefore, there is still a need for further research on degradable biomaterials as delivery systems. Moreover, the elimination and management of antibiotic-resistant bacteria associated with multidrug resistance (MDR) is a growing problem in healthcare institutions due to persistent nosocomial infections.[9] An example of this healthcare concern is *Acinetobacter baumannii* (*A. baumannii*); this bacterium evolved from a harmless epithelial bacterium to an MDR bacterium frequently associated with pernicious wound healing infections.[10] Immunocompromised patients with bacteremia, which, in some cases, develops from infected wounds, may evolve into pneumonia, septicemia, and urinary tract infections. Infections with MDR bacteria often lead to complications, including delayed wound healing, skin graft failure, sepsis, and amputation.[11] Furthermore, *A. baumannii* is resistant to

Received: August 23, 2023
Revised: December 21, 2023
Accepted: December 25, 2023
Published: January 3, 2024

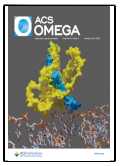

metal salts, which limits treatment options and increases mortality. Its clinical relevance ranks first on the list of six priority pathogens (ESKAPE) of the Infectious Diseases Society of America.[12−14] Additionally, cancer patients and end-stage patients with multiorgan failure are more likely to develop chronic nonhealing wounds.[4,15] Management of chronic nonhealing wounds will be palliative to improve the patient's quality of life and control bleeding, odor, pain, exudate, and superficial infection.[16,17]

Active ingredients with antimicrobial effects can be incorporated into dressings, such as silver nanoparticles (AgNPs), for release into the wound.[8,18] Alginate, a polysaccharide obtained from brown algae, has been approved for biomedical use in drug delivery and tissue engineering due to its biocompatibility and biodegradability.[19] Alginate aerogels can absorb large volumes of exudate and form a gel that concentrates in the wound area.[20,21] Additionally, calcium alginate aerogels are used as topical hemostatic agents to stop bleeding from malignant wounds. Calcium alginate dressings are recommended to reduce moist peeling because of treatment with radiotherapy and cetuximab, as an early application in head and neck cancer, or they can be impregnated with AgNPs to treat wounds with beneficial effects related to the control of exudates and the sustained release of antimicrobial agents.[22,23] Electrospinning-based alginate-AgNP dressings have a gauze-like structure, showing antibacterial and hemostatic activity.[24] Furthermore, AgNPs coated with α-lipoic acid (ALA), an antioxidant compound, have shown reduced toxicity and anti-inflammatory activity compared to uncoated AgNPs.[25] Therefore, while AgNPs decrease bacterial growth, virulence, and biofilm-related gene expression of *A. baumanni* from wound infections,[26] ALA can be administered to reduce the inflammatory state, while AgNPs can control bacterial infections in wounds. However, alginate-based dressings have poor structural stability.[27] Therefore, strategies like plasticization have been used to reduce intermolecular attractive forces between polymer chains and improve the structural stability of alginate-based aerogels.[28,29] Moreover, the transdermal delivery of ALA in a poly(ethylene glycol)-plasticized aerogel is improved.[30] Thus, alginate aerogels can be designed to control bleeding, exudate, and superficial infection and to deliver molecules. Previous works have reported on dressings with silver nanoclusters and have evaluated the synergistic effects between alginate and silver;[31] however, the goal of our work was to provide a material with improved features of hemocompatibility, antioxidant, and anti-inflammatory properties that also possess antimicrobial activity against the MDR *A. baumannii*. Based on the above information, we have designed aerogels made up of alginate to contain and deliver silver nanoparticles, which are coated with α-lipoic acid (AgNP-ALA). Alginate has the role of containing AgNP-ALA. AgNPs are the vehicle for ALA to be delivered since AgNPs are functionalized with ALA. To reduce the intermolecular attraction forces between polymers chains, and therefore increase the handling and stability to aqueous medium of our alginate-based aerogels, we added poly(ethylene glycol) methyl ether methacrylate (PEGMA) as a plasticizer.[31] AgNPs-ALA possesses the capacity to neutralize, or scavenge, free radicals like reactive oxygen species, ROS, a defense mechanism against an invading microbe and $NO^{\bullet}$, a pro-inflammatory mediator.[32] Both, ROS and $NO^{\bullet}$, have detrimental effects on wound healing when produced and released at high levels during pathological conditions. Therefore, our aerogels containing lipoic acid-capped AgNPs would enhance wound healing given their free radical scavenging and antimicrobial properties. The proposed aerogels have antimicrobial activity against the MDR *A. baumannii* and improved features of hemocompatibility, antioxidant, and anti-inflammatory capacities compared to a commercial material, which demonstrates their potential application in biomedicine.

2. MATERIALS AND METHODS

2.1. Materials. Reagents used for this research were purchased from Sigma-Aldrich, Mexico. Aerogels were synthesized by adding PEGMA Mn ∼500 (Cat. no. 447943) to alginic acid sodium salt—with a molecular weight of 120,000−190,000 g/mol and a mannuronic acid/guluronic acid ratio (M/G) of 1.56 (Cat. no. 180947) and calcium chloride ($CaCl_2$). Commercial AgNPs, functionalized with α-lipoic acid (AgNPs-ALA), (Cat. no. 807370) were incorporated into the aerogel mix solution. To evaluate the antioxidant and anti-inflammatory activities, the following reagents were used: sodium persulfate (KPS) (Cat. no. 216224); 2,2′-azinobis(3-ethylbenzothiazoline-6-sulfonic acid) ($ABTS^{\bullet+}$) (Cat. no. 11684302001); (±)-6-Hydroxy-2,5,7,8-tetramethylchromane-2-carboxylic acid (Trolox) (Cat. no.238813); sodium nitroprusside (SNP) dihydrate (Cat. no.71778); and Griess 1× Reagent (Cat. no. G4410). Furthermore, to evaluate aerogel biocompatibility using resazurin (GoldBio, Cat. no. R-110), the HFF1 fibroblast cells (Cat. no. SCRC-1041) from the American Type Culture Collection (ATCC) were grown in D-MEM F12 medium (Cat. no. D6434), supplemented with 10% fetal bovine serum (Cat. no. F2442) and 1% antibiotic/antimycotic (Cat. no. A5955), and trypsin/EDTA (Cat. no. 59417C), all obtained from Sigma-Aldrich, Mexico. For bactericidal assays, *Escherichia coli* (ATCC 25922) and a clinical isolate of *Acinetobacter baumanii* strain were donated by Centro de Investigación Biomédica de Occidente, Instituto Mexicano del Seguro Social (CIBO, IMSS) diluted in saline solution (0.85% NaCl, MERCK 1.06404.0500). Bacterial growth was maintained with MH agar plates (BD-BIOXON Cat. no. 211667), blood agar (BD, Cat. no. 220150), tryptic soy broth (BD-BACTO, Cat. no. 211825) with glycerol (Sigma-Aldrich, Mexico, Cat. no. G2025), while the antibiotics gentamycin (Cat. no. G1264), polymyxin B (Cat. no. P4932), trimethoprim (Cat. no. 92131), and tobramycin (Cat. no. T4014) were obtained from Sigma-Aldrich, Mexico, and ampicillin (Cat. no. 10045) was obtained from Fluka. Finally, CVS Health Sterile Antimicrobial Silver Alginate Dressing was used as a commercial control (CD, commercial dressing).

2.2. Synthesis of Aerogels. Aerogels were prepared from sodium alginate solution 3% (w/v) mixed with PEGMA to obtain final concentrations of 1.5% (w/v) and 0.375% (v/v), respectively. The alginate solution was cross-linked with calcium ions by adding chloride calcium solution 1.5% (w/v) in equal parts (v/v). The solution was then stirred to obtain a homogenized Ca-Alg-PEGMA solution,[29,33] Aerogels were prepared with concentrations of AgNPs higher than 0.025 μg/mL, as has been reported.[34] The AgNPs-ALA concentrations of 0.025 and 0.0375 μg/mL were incorporated into the Ca-Alg-PEGMA solution. The final concentrations were 7.5 μg (7.5 NP) and 11.25 μg (11.25 NP) per aerogel. A sample of 0.6 mL of each solution was poured onto 24-well plates and frozen for 48 h, followed by freeze-drying (Labconco FreeZone, 1L) for 24 h (Figure 1).

https://doi.org/10.1021/acsomega.3c06114
ACS Omega 2024, 9, 2350−2361

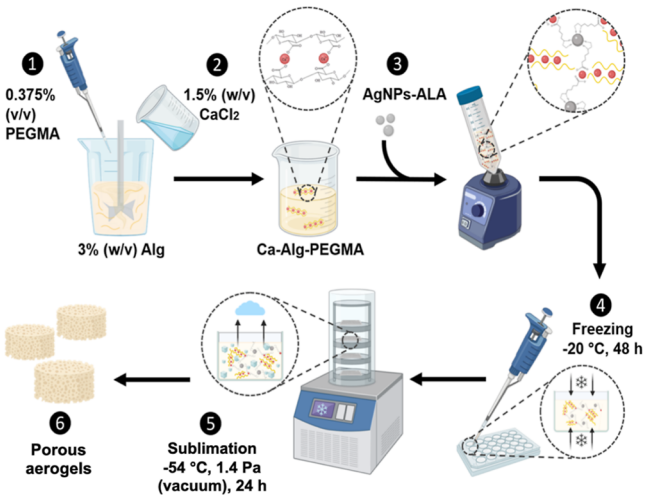

Figure 1. Schematic representation of the preparation process of alginate-based aerogels with α-lipoic acid-capped silver nanoparticles (AgNP-ALA). (1) PEGMA was added to a sodium alginate solution to final concentrations of 0.375% (v/v) and 1.5% (w/v), respectively. (2) $CaCl_2$ was added dropwise to the Alg-PEGMA mixture to a final concentration of 0.75% (w/v), while stirring. (3) AgNP-ALAs were added to the already cross-linked Alg-PEGMA solution to obtain a final concentration of 7.5 and 11.25 μg per aerogel. (4) The Alg-PEGMA-AgNP-ALA mixture was poured into polystyrene molds, frozen at −20 °C for 48 h, and then (5) freeze-dried for 24 h to obtain porous alginate-based aerogels with AgNP-ALA (6). Image by authors.

2.3. Microscopic and Spectroscopic Characterization. The structures of the surfaces of aerogels and commercial dressing were imaged via a scanning electron microscopy (SEM) instrument EVO/MA15 ZEISS at 15 kV accelerating voltage and variable pressure. The chemical composition of the aerogels was analyzed by energy-dispersive X-ray (EDX) microanalysis and an FT-IR spectrophotometer (Agilent Cary 630, ATR cell) from 500 to 4000 cm^{-1}. X-ray computed tomography (μCT) imaging was performed with a SkyScan 2211. The high-resolution nano-CT scanner (Bruker, Belgium) was equipped with a 190 kV/50 μA^{-1} mA tungsten X-ray source and an 11-megapixel (4032 × 2670) X-ray-sensitive CCD detector. Samples were scanned using 110 kV accelerating voltage and target current of 250 μA, using a 0.5 μm copper source target, with full 360 sample rotation (0.20 increment) and an exposure time of 1500 ms per frame and pixel size of 1 μm. Reconstruction was performed using Bruker's NRecon software version 1.7. Subsequent 3D morphometric analyses were conducted using Bruker's CTAn software version 1.20.

2.4. Determination of Antioxidant Activity. $ABTS^{\bullet+}$ was produced due to the reaction between an ABTS stock solution with 0.87 mM potassium persulfate (KPS) in a 1:1 ratio. The ABTS/KPS solution was left in a dark place at 22 °C for 18 h before use. The $ABTS^{\bullet+}$ solution was diluted with distilled water until an absorbance of 0.70 ± 0.2 at 734 nm was obtained. The aerogels and commercial dressing were cut into 6 pieces and immersed in 900 μL of $ABTS^{\bullet+}$. After 6 min of incubation in the darkness, 200 μL were transferred to a 96-well plate, and absorbance was recorded at 734 nm (Epoch, BioTek).[35] The percentage of inhibition was calculated by the formula

$$\text{inhibition, \%} = \frac{\text{Abs}_{\text{control}} - \text{Abs}_{\text{sample}}}{\text{Abs}_{\text{control}}} \times 100$$

where $\text{Abs}_{\text{control}}$ is the absorbance of $ABTS^{\bullet+}$ and water and $\text{Abs}_{\text{sample}}$ is that of $ABTS^{\bullet+}$ and the aerogel. A reference curve was prepared using Trolox at different concentrations (0−120 nmol/mL) prepared with absolute ethanol.[29,35] The inhibition of $ABTS^{\bullet+}$ by the aerogels was compared against the Trolox standard, and the results were expressed in terms of nanomoles of Trolox equivalent antioxidant capacity (TEAC) per mg of aerogel.

2.5. Determination of Anti-Inflammatory Activity. The SNP assay was adapted to determine the anti-inflammatory activity, related to the $NO^{\bullet}$ scavenging capacity of the aerogels.[36,37] The aerogels and commercial dressing were cut into 6 pieces, immersed in 1200 μL of 2.5 mM SNP, and incubated for 1 h in light. A sample of 100 μL of each condition was transferred to a 96-well plate, and 100 μL of 1× Griess Reagent was added and incubated for 15 min in dark conditions at 22 °C. The $NO^{\bullet}$ scavenging was determined by the absorbance at a wavelength of 540 nm (Epoch, BioTek) using the following formula

$$NO^{\bullet}\ \text{scavening, \%} = \frac{\text{Abs}_{\text{control}} - \text{Abs}_{\text{sample}}}{\text{Abs}_{\text{control}}} \times 100$$

where $\text{Abs}_{\text{control}}$ is the absorbance of 1× Griess Reagent with SNP and $\text{Abs}_{\text{sample}}$ is the absorbance of 1× Griess Reagent with SNP and the aerogel. A reference curve was obtained using indomethacin at different concentrations (50−200 nmol mL^{-1}) prepared with absolute methanol. The $NO^{\bullet}$ scavenging effect determined from each aerogel was compared to the values obtained from the indomethacin curve. The results were expressed in terms of nanomoles of indomethacin equivalent anti-inflammatory capacity (IEAC) per mg of aerogel.

2.6. Hemocompatibility. The aerogels and commercial dressing were put into contact with blood from healthy donors to determine the compatibility in terms of hemoglobin release.[38] The blood was collected in a BD vacutainer with sodium citrate. The aerogels were first incubated for 30 min at 37 °C with 500 mL of 1× PBS. Subsequently, 20 mL of blood was added to the aerogels, water was used as the positive control, and 1× PBS was used as the negative control instead of aerogels. After incubating the samples for 60 min at 37 °C, they were centrifuged at 700*g* for 10 min at 22 °C. A 200 mL portion of each sample was transferred to a 96-well plate to read absorbance at a wavelength of 540 nm (Epoch, BioTek). The percentage of hemolysis was calculated via the following equation

$$\text{hemolysis, \%} = \frac{\text{Abs}_{\text{sample}} - \text{Abs}_{\text{negative control}}}{\text{Abs}_{\text{positive control}} - \text{Abs}_{\text{negative control}}} \times 100$$

The blood sampling was approved by the Bioethics Committee of the Center for Scientific Research and Higher Education at Ensenada (CICESE) (CBE/PRES-O/004).

2.7. Cell Viability. HFF1 fibroblast cells were used to analyze the biocompatibility of aerogels. This effect was determined via the conversion of resazurin to resorufin. Cells were grown in D-MEM F12 medium supplemented with 10% FBS and 1% antibiotic/antimycotic. The cells were maintained in a T25 flask at 37 °C in a 5% CO_2 atmosphere. Once confluent, the monolayer was enzymatically detached for 1 min at 37 °C with 500 μL of trypsin/EDTA and D-MEM F12

https://doi.org/10.1021/acsomega.3c06114
ACS Omega 2024, 9, 2350−2361

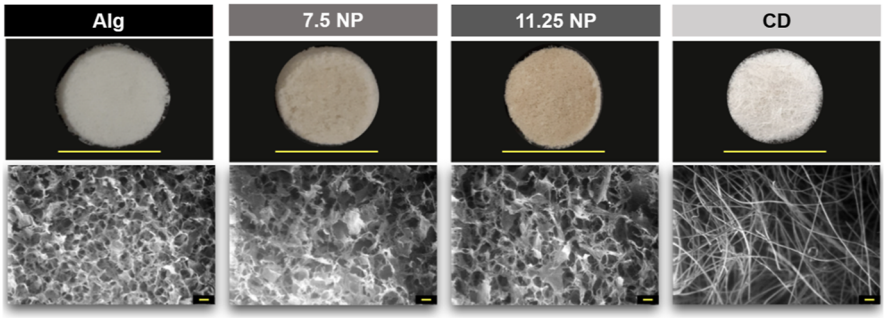

Figure 2. Morphological characterization of alginate-based aerogels with α-lipoic acid-capped silver nanoparticles (AgNP-ALA). The morphological characteristics of aerogels did not change as AgNP-ALA was added into biocomposites. Semispherical and interconnected pores are visible in our synthesized aerogels. The commercial dressing shows a fibrous, nonwoven, microstructure. Alg: calcium alginate-PEGMA aerogel. 7.5 NP: calcium alginate-PEGMA aerogel containing 7.5 μg of AgNP-ALAs per aerogel. 11.25 NP: calcium alginate-PEGMA aerogel 11.25 μg of AgNP-ALAs per aerogel. CD: commercial silver alginate dressing. Scale bars: 10 mm for pictures and 100 μm for SEM images. Photographs were provided by authors.

supplemented medium was added. Then, aerogels with 100,000 cells per well were placed into a 48 well-plate and incubated for 24 h at 37 °C in a 5% CO_2 atmosphere. After 24 h of incubation, 500 μL of 10× resazurin diluted 1:2 solution was added and incubated for 2 h under standard conditions. Controls of our cell-free materials were included to prevent the impact of chemical interactions with resazurin on the results. The supernatant was transferred to a 96-well ELISA plate. The absorbance was measured at 570 and 600 nm in an ELISA plate reader (xMark Microplate Spectrophotometer, BioRad). The resazurin-resorufin reduction percentage was determined by the next formula

$$\text{resazurin} - \text{resurafin reduction, \%} = \frac{[(117{,}216)(A570\text{ nm})] - [(80{,}586)(A600\text{ nm})]}{[(155{,}677)(A'600\text{ nm})] - [(14{,}652)(A'570\text{ nm})]} \times 100$$

where 117,216 = molar extinction coefficient of the oxidized form of the dye 600 nm; 80,586 = molar extinction coefficient of the oxidized form of the dye 570 nm; 155,677 = molar extinction coefficient of the reduced form of the dye 570 nm; 14,652 = molar extinction coefficient of the reduced form of the dye 600 nm.

Finally, cell survival was calculated against the positive control (cells without treatment) using the following formula

$$\text{survival, \%} = \frac{\text{percentage of reduction from each treatment}}{\text{percentage of reduction of control}} \times 100$$

2.8. Bacterial Viability in PBS as a Vehicle for Antibacterial Assays and the Antibiotic Disk Diffusion Method. The bacterial viability of *E. coli* ATCC 25922 and the MDR *A. baumanii* was determined by maintaining at different times the strains in PBS as a vehicle for further assays. Initially, a working aliquot from each strain was seeded on MH agar and incubated for 18 h at 35.5 ± 1.0 °C. Then, a suspension of each bacterial strain was prepared, with 1.0 ± 0.5 × 10^6 colony-forming units per mL (cfu/mL) in 1× PBS and incubated at 0, 24, 48, 72, and 96 h at 25 ± 3.0 °C. Bacterial viability was determined using 100 μL of a bacterial suspension at different incubation times, using the viable count assay. The antibiotic susceptibility for both strains, *E. coli* and *A. baumannii*, was determined by disk diffusion assay following The Clinical and Laboratory Standards Institute in the M02-A10 document, with some modifications,[39] and considering that *A. baumanii* was isolated from a hospital collection. Briefly, a bacterial suspension was prepared in saline buffer, and the inoculum density was adjusted to a standard turbidity equivalent to the 0.5 McFarland standard; the bacterial suspension was plated with a swab on a 90 mm plate with MH agar. Once the suspension dried on the surface of the MH agar, a 6 mm disk previously impregnated with 10 μL of different antibiotics was distributed equidistantly on the plate. The antibiotics analyzed were gentamicin (10 or 160 μg), polymyxin B (20 μg equivalent to 300 U), trimethoprim (5 μg), ampicillin (10 μg), and a mixture of gentamicin (10 μg) with polymyxin B (20 μg equivalent to 300 U) or tobramycin (10 μg) with polymyxin B (20 μg equivalent to 300 U). The plates were then incubated for 20 h at 35.5 ± 1.0 °C and the zones of inhibition (ZOIs) were measured in mm. The same protocol was followed for the analysis of *E. coli*. All assays were performed in duplicate.

2.9. Bactericidal Effect of Aerogels on Bacterial Strains. The bactericidal effect of the 7.25 NP and 11.5 NP aerogels was determined by a dilution method, using *E. coli* (ATCC, 25922) as the reference control and *A. baumanii* as an MDR strain. Both strains were resuspended and maintained in PBS for up to 96 h, as previously indicated in Section 2.8. Previously, the original strains were grown on blood agar at 37 °C for 18 h. Then, working aliquots (WA) filled with cryopreservation medium containing 10% glycerol and tryptic soy broth were kept at −70 °C until use. Before each bactericidal assay, one WA of each strain was spread on an MH agar plate and incubated at 35.5 ± 1.0 °C for 18 h. The assay was started by resuspending the strains in 1 mL of 1× PBS at a setting of 1.9 ± 0.5 × 10^6 cfu/mL and each aerogel, i.e., Alg, 7.5 NP, 11.25 NP, and CD, was added individually to the bacterial suspension. Polymyxin B at 2 μg (300 U) was used as a control based on the previous susceptibility determination of the *A. baumanii* strain. Finally, the bacterial viability was determined by the plate dilution method after 0, 2, 24, 48, 72, and 96 h of incubation of the bacterial suspension in PBS with each aerogel at 25 ± 3.0 °C. To do this, serial dilutions (10^{-1} to 10^{-4}) of the bacterial suspension were seeded on duplicate MH agar plates and incubated at 35.5 ± 1.0 °C for 24 and 48 h. Colonies were counted after 48 h of incubation at 35.5 ± 1.0 °C. All assays were performed in triplicate on three different days.

https://doi.org/10.1021/acsomega.3c06114
ACS Omega 2024, 9, 2350−2361

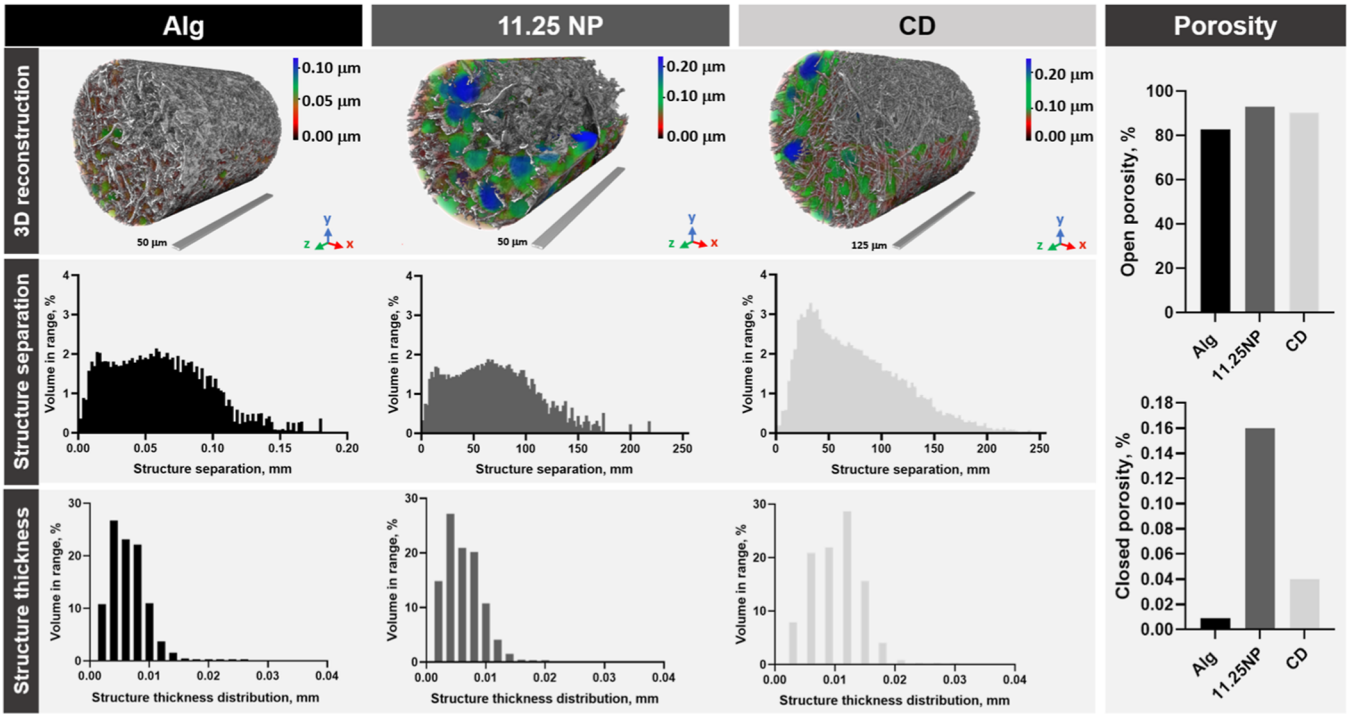

Figure 3. Morphometric characterization of alginate-based aerogels with α-lipoic acid-capped silver nanoparticles (AgNP-ALA). Alg: calcium alginate-PEGMA aerogel. 11.25 NP: calcium alginate-PEGMA aerogel 11.25 μg AgNP-ALAs per aerogel. CD: commercial silver alginate dressing. Three-dimensional reconstruction by μCT of aerogels. The pore structure separation distribution increased when AgNPs were incorporated into the matrix. The pore structure thickness distribution was similar between our aerogels, but the CD pore thickness was higher. All three showed a high percentage of interconnected pores that were tunnel-like and a low percentage of dead-end cavities.

2.10. Statistical Analysis. Data were analyzed with GraphPad Prism version 8. Antioxidant activity, $NO^{\bullet}$ scavenging, antimicrobial activity, cell viability, hemocompatibility, and bactericidal assays are shown as the mean ± standard deviation (SD) of at least three independent experiments. Statistical analysis was performed by one-way ANOVA with Tukey's multiple comparisons posthoc test. Blood coagulation assay is presented as mean ± standard deviation (SD) of at least three independent experiments. Statistical analysis was performed by two-way ANOVA with Sidak's multiple comparisons posthoc test. The significance criterion in the statistical analysis was set at $p < 0.05$. Asterisks indicate statistical difference *($p < 0.05$), **($p < 0.01$), ***($p < 0.001$) and ****($p < 0.0001$).

3. RESULTS AND DISCUSSION

3.1. Morphological and Physicochemical Characterization of Aerogels. The topography of aerogels directly affects the behavior of cells in their orientation, migration, and production of cytoskeletal elements.[40] SEM was used to analyze the microstructure of the external surface morphology of the aerogels (Figure 2). The pore structure of our synthesized aerogels revealed a highly porous and interconnected architecture, whereas the commercial dressing had a nonwoven fibrous matrix that is related to its electrospinning synthesis. An interconnected and porous network enhances cell seeding in the materials and leads to cell infiltration and tissue growth.[41] Since SEM does not provide quantitative information on porosity, the distribution and interconnectivity of pores within the sample were investigated by using X-ray computed tomography (Figure 3). Computer-generated 3D images allowed quantification of pore structure separation and thickness distribution. The structure separation analysis indicated that Alg aerogels showed a pore size range distribution of 0−100 μm, with a higher percentage around 10 μm. The 11.25 NP aerogels showed a uniformly distributed pore size distribution between 2 and 218 μm and a structural separation of 110 ± 63.21 μm. The CD had a pore size range distribution of 0−225 μm, with a higher percentage around 30−39 μm (12.6%) and a structure spacing of 132 ± 75.77 μm. Pores smaller than 160 μm allow migration and proliferation of dermal fibroblasts.[42] Endothelial infiltration promotes angiogenesis, and the diffusion of cellular nutrients and waste products requires a minimum porosity of 30−40 μm.[43] Pores between 160 and 200 μm promote the formation of new vessels along aerogels.[44]

Our aerogels had a similar structure thickness distribution: at a 0.004 mm thickness, Alg (26.67%) and 11.25 NP (27.19%) had the highest percentage, whereas CD had a broad thickness distribution at 0.012 mm (28.68%). The thickness of the Alg structure is 0.014 ± 0.007 mm, 11.25 NP is 0.0165 ± 0.009 mm, and CD is 0.011 ± 0.006 mm. All of these structures presented high percentages of open cavities 82.6% for Alg, 92.9% for 11.25 NP, and 90.2% for CD, plotted as open porosity, while the percentage of dead-end cavities was less than 0.01% Alg, 0.16% 11.25 NP, and 0.04% CD, represented as closed porosity. A highly porous structure with thin walls was observed. These results confirm the SEM micrographs, which show an extensive and interconnected porous network throughout its structure. Thus, our aerogels achieved the architecture required to provide biomechanical support to grow cells and allow metabolite exchange.

To investigate the chemical interactions and to identify the functional groups, aerogels were characterized by FT-IR

https://doi.org/10.1021/acsomega.3c06114
ACS Omega 2024, 9, 2350−2361

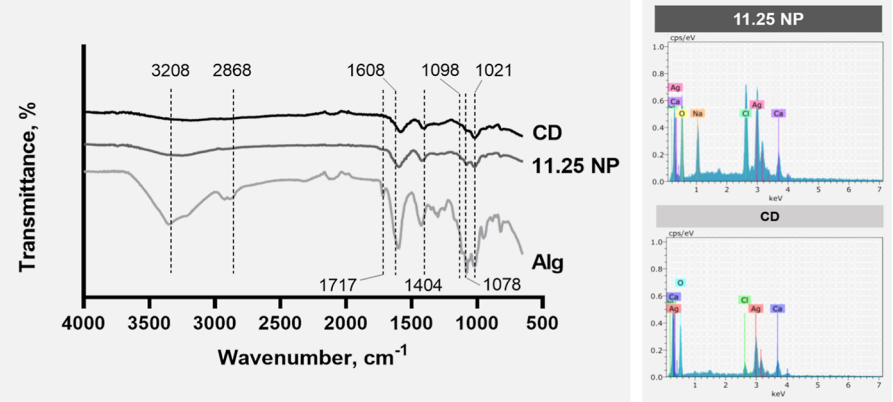

Figure 4. Chemical characterization of alginate-based aerogels with α-lipoic acid-capped silver nanoparticles (AgNP-ALA). (a) FT-IR spectra show the different alginate aerogels in the regions of 1000−1800 cm^{-1} and 2800−3200 cm^{-1}. (b) EDX of 11.25 NP and CD aerogels shows their elemental composition and the presence of Ag incorporated into the matrix. Alg: calcium alginate-PEGMA aerogel. 11.25 NP: calcium alginate-PEGMA aerogel 11.25 μg AgNP-ALAs per aerogel. CD: commercial silver alginate dressing.

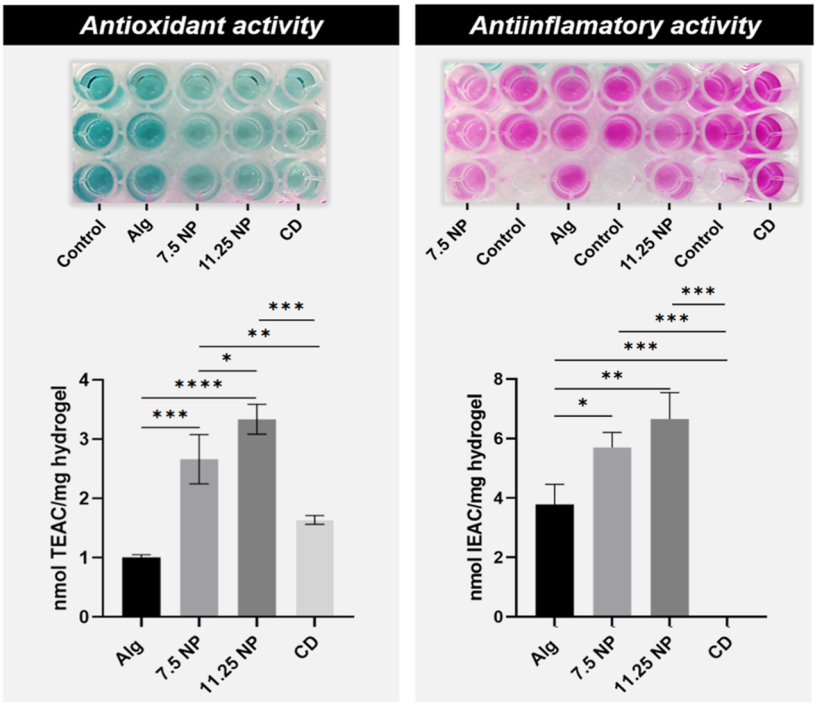

Figure 5. In vitro antioxidant and anti-inflammatory activity of alginate-based aerogels with α-lipoic acid-capped silver nanoparticles (AgNP-ALA). Free radical scavenging activity is expressed as nanomoles of TEAC per mg of aerogel due to their capacity to inhibit $ABTS^{\bullet+}$ oxidation. Anti-inflammatory activity is expressed as Indomethacin equivalent anti-inflammatory capacity per milligram of aerogel, in terms of their capacity of nitric oxide radical ($NO^{\bullet}$) scavenging. Data are presented as mean ± SD, $n = 3$ per group, *$p < 0.05$, ***$p < 0.001$, ****$p < 0.0001$, by one-way ANOVA and Tukey's multiple comparison posthoc. Alg: calcium alginate-PEGMA aerogel, 7.5 NP: calcium alginate-PEGMA aerogel containing 7.5 μg AgNP-ALAs per aerogel. 11.25 NP: calcium alginate-PEGMA aerogel 11.25 μg AgNP-ALAs per aerogel. CD: commercial silver alginate dressing. Control: blank ($ABTS^{\bullet+}$ with water, for antioxidant activity; SNP with water, for $NO^{\bullet}$ scavenging). Photographs by authors.

analysis (Figure 4). The FT-IR spectra of Alg, 11.25 NP, and CD showed their assignments of the characteristic vibrational modes, with dotted lines. The alginate O−H bond is shown at 3208 cm^{-1} of the Alg spectrum. When AgNPs-ALA are incorporated into the alginate matrix, this peak appears flattened in the 11.25 NP spectrum. The symmetric vibrations of the COO^{-} group were found at 1404 cm^{-1}, which is present in all three spectra as they are composed of alginate.[29] Both 1078 and 1021 cm^{-1} peaks are attributed to the stretching vibration of the C−O−C bond of the ring of alginate monomers.[45] When there is a metal−carboxylate interaction, the vibrations are weakened,[46] as is shown in 11.25 NP and CD spectra. The characteristic PEGMA peak at 2868 cm^{-1} corresponds to the stretching of the C−H of the $-CH_3$ group; this peak is only expected in our Alg-PEGMA aerogels. The 1717 cm^{-1} peak is attributed to the C═O stretching from PEGMA in the Alg aerogel spectrum, confirming the incorporation of PEGMA in Ca-Alg-PEGMA.[29] To stabilize the alginate egg-box model, the metal atom interacts with one oxygen of its two adjacent C═O groups in polyguluronic acid chains.[47] However, in this case, given that AgNPs are covered by lipoic acid, the interactions between the nanoparticles and

https://doi.org/10.1021/acsomega.3c06114
ACS Omega 2024, 9, 2350−2361

the polymeric matrix could be attributed to the carboxylate groups of lipoic acid with calcium cations in the calcium alginate network.[46]

The similarity between the 11.25 NP and CD spectra is due to the AgNPs interacting with the alginate monomers. The elemental composition of the solids on the surface by EDX was determined (Figure 4) for 11.25 NP and CD. Our aerogels were obtained by mixing sodium alginate with calcium chloride, so the EDX spectrum of 11.25 NP revealed the peaks of the synthesis elements Ca, Na, Cl, and O, while the CD spectrum only presents peaks of Ca, Cl, and O. Both aerogels show a strong signal in the silver region at 3 keV,[48,49] which confirms the results of the FT-IR of AgNPs' incorporation into the calcium alginate matrix. The microstructure and surface chemistry play an important role in the biological reactions of biomaterial surfaces;[50,51] therefore, we expect that properties such as antioxidant, anti-inflammatory, antimicrobial activities, hemocompatibility, and blood clotting will be influenced by those characteristics.

3.2. Antioxidant and Anti-Inflammatory Activities. Excessive amounts of ROS can cause a cellular imbalance in the reduction−oxidation reactions and disrupt normal biological functions, leading to oxidative stress, which generates cell damage due to the oxidation of molecules, mutagenesis, cell death, inflammation, and carcinogenesis.[52] α-Lipoic acid is a thiol antioxidant, the precursor of glutathione (GSH), vitamin C, and E. In the reduced form it can react with free radicals; therefore, it can regulate the inflammatory response.[53,54] Moreover, PEGMA due to its C═C double bond can also contribute to the radical scavenging properties of our aerogels.[55,56] To determine the antioxidant capacity of our aerogels, they were placed in contact with the $ABTS^{\bullet+}$ solution, and the ability to inhibit the oxidation of the radical was measured, at 734 nm.[35] The antioxidant activity was expressed as Trolox equivalent antioxidant capacity (TEAC), determined by using as reference Trolox, a synthetic analog of vitamin E (Figure 5).[57] The antioxidant activity of aerogels increased from 1 ± 0.043 nmol TEAC/mg per aerogel in Alg to 2.66 ± 0.415 nmol de TEAC/mg per aerogel for 7.5 NP (2.6-fold) and 3.33 ± 0.25 nmol de TEAC/mg per aerogel for 11.25 NP (3.3-fold), while CD had 1.64 ± 0.072 nmol TEAC/mg per aerogel. Our AgNP-ALA-containing aerogels have an increased antioxidant activity instead of the commercial dressing, which has 13 times more silver than 11.25 NP aerogels. Based on this, our aerogels exhibit a significant in vitro behavior, which could be effective in neutralizing ROS and pro-inflammatory molecules, to re-establish the positive influence that low ROS levels can have as antibacterial and cell signaling messenger, in the recruitment, migration, proliferation, and differentiation of cells. Inflammation is a physiological process in response to harmful stimuli resulting from pathogen infection, chemical irritation, and/or tissue damage.[58] During this process, severe molecules are released as pro-inflammatory cytokines and free radicals. Nitric oxide radical ($NO^{\bullet}$) is a pro-inflammatory mediator involved in immunological processes such as fighting bacterial infections and tumors or wound healing. When $NO^{\bullet}$ is released at high levels during pathological conditions, it triggers tissue inflammation.[32] $NO^{\bullet}$ concentrations of 30−100 nM have been related to a pro-tumorigenic state and identified as a poor prognostic indicator.[59] The anti-inflammatory activity was determined by the capacity of the aerogels to scavenge $NO^{\bullet}$, donated by SNP.[37] The amount of $NO^{\bullet}$ was measured with the 1× Griess Reagent, which reacts with SNP to produce a pink-colored solution with a wavelength of 540 nm (Figure 5). All aerogels have activity related to $NO^{\bullet}$ scavenging. The Alg aerogel showed 18.22% of $NO^{\bullet}$ scavenging, and it has been previously reported that PEG has anti-inflammatory properties;[60] therefore, this property can be attributed to the PEGMA incorporation.[29] In the case of 7.5 and 11.25 NP, these showed 30.4 and 37.47% of $NO^{\bullet}$ scavenging, respectively. Meanwhile, the commercial dressing did not have the capacity to scavenge the $NO^{\bullet}$ at all. Increased amounts of nitric oxide synthase and superoxide dismutase have been reported in chronic wounds during nonhealing processes. Thus, our results show that the antioxidant and anti-inflammatory capacities of the aerogels increase as the AgNP-ALA concentration increases. Acute inflammation and oxidative stress can lead to chronic inflammation; therefore, it is suitable to assume that AgNP-ALA can modulate these processes with the combined radical scavenging and anti-inflammatory activities of aerogels.

3.3. In Vitro Biocompatibility. The cytocompatibility of the aerogels was determined in human fibroblasts after 24 h of incubation. Fibroblast survival increased statistically significantly when seeded into the aerogels. The used AgNP concentration did not affect the cell viability as has been reported with concentrations higher than 5 μg/mL of AgNPs ALA-capped (Figure 6).[25] The percentage of hemolysis below

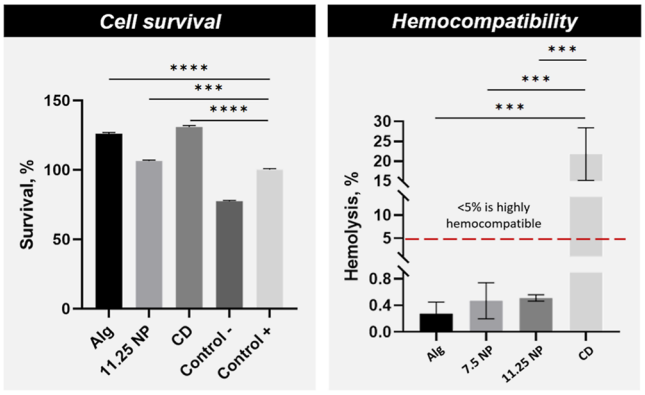

Figure 6. In vitro biocompatibility of alginate-based aerogels with α-lipoic acid-capped silver nanoparticles (AgNP-ALA). Human fibroblasts HFF-1 cell viability was determined by resazurin to resorufin percentage after 24 h of incubation with the 11.25 NP aerogel and is expressed as a percentage (%). Absorbance of hemoglobin released from erythrocytes of blood samples incubated with aerogels for 60 min at 37 °C is presented as a percentage. Data are presented as mean ± SD, n = 3 per group, *p < 0.05, ***p < 0.001, ****p < 0.0001, by one-way ANOVA and Tukey's multiple comparison posthoc. Alg: calcium alginate-PEGMA aerogel. 7.5 NP: calcium alginate-PEGMA aerogel containing 7.5 μg AgNP-ALAs per aerogel. 11.25 NP: calcium alginate-PEGMA aerogel 11.25 μg AgNP-ALAs per aerogel. CD: commercial silver alginate dressing. Control (+): cells without any treatment, control (−): cells with 50% DMSO; (for survival assay). Control (+): water, control (−): PBS 1×; (for hemolysis assay).

5% establishes one of the criteria to demonstrate the hemocompatibility of biomaterials, according to ISO 10993-1,[38] indicating if the material can cause the lysis of erythrocytes and the subsequent hemoglobin release. To prove the hemocompatibility of aerogels, they were incubated with blood from healthy volunteers. The percentage of hemolysis was Alg 0.28%, 7.5 NP 0.47%, and 11.25 NP 0.51%, while the

https://doi.org/10.1021/acsomega.3c06114
ACS Omega 2024, 9, 2350−2361

A)

Strain	Bacterial load in PBS after incubation at 25±3.0°C (CFU/mL)				
	0h	24h	48h	72h	96h
E. coli ATCC 25922	627,500	117,750	67,250	92,250	199,000
A. baumanii	1,007,500	930,000	1,162,500	1,080,000	1,107,500

B)

Antibiotic disk	Inhibition zone diameter (mm)		
	Strain (average diameter)		Expected results for *E. coli* (ATCC 25922)*
	A. baumanii	*E. coli* (ATCC 25922)	
Gentamicin 10µg	6.0 (R)	20.3	19-27
Tobramycin 10 µg	6.7 (R)	19.3	18-26
Polymyxin 300U	15.8 (NA)	17.8	13-19
Ampicillin 10 µg	6.0 (R)	15.8	15-22
Trimethoprim 5 µg	6.0 (R)	27.0	21-28
+ Gentamicin 10 µg with Polymyxin 300U	15.7	17.7	NA
+ Gentamicin 160µg	11.3	25.3	NA
+ Tobramycin 10 µg with Polymyxin 300U	16.3	18.7	NA
+ Tobramycin 160 µg	13.7	24.3	NA

+, NA: Not previously evaluated according to the CLSI (2016).
R: Resistant, according to Table 2B from CLSI, 2016.
*According to CLSI, 2016.

c)

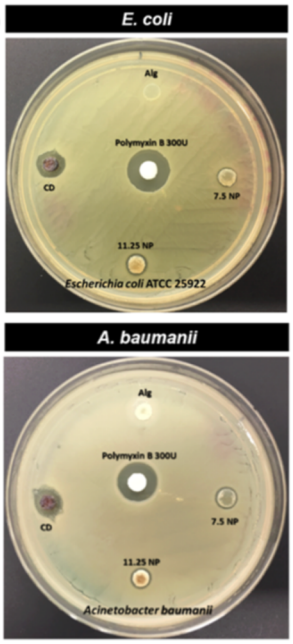

Figure 7. Disk diffusion test for *A. baumanii* and *E. coli*. (a) Bacterial viability on 1× PBS as a vehicle for the assays. (b) Antibiotic susceptibility disk diffusion assay for MDR *A. baumanii* and the reference bacterium *E. coli* ATCC25922. Mueller Hinton Agar on the 90 mm plate was inoculated with an adjusted suspension (turbidity equivalent to a 0.5 McFarland standard) The table shows the ZOI expressed by diameter in mm, when a disk with antibiotic was placed on the surface. (c) Antibiotic disks and aerogels were placed on the surface of the previously inoculated medium, and the amount of antibiotic, or mix of them, were deposited in each disk in 10 μL of PBS, as diluent. The above representative photographs show the ZOI after 20 h of incubation at 35.5 ± 1 °C. Alg: calcium alginate-PEGMA aerogel. 7.5 NP: calcium alginate-PEGMA aerogel containing 7.5 μg AgNP-ALAs per aerogel. 11.25 NP: calcium alginate-PEGMA aerogel 11.25 μg AgNP-ALAs per aerogel. CD: commercial silver alginate dressing. Photographs by authors.

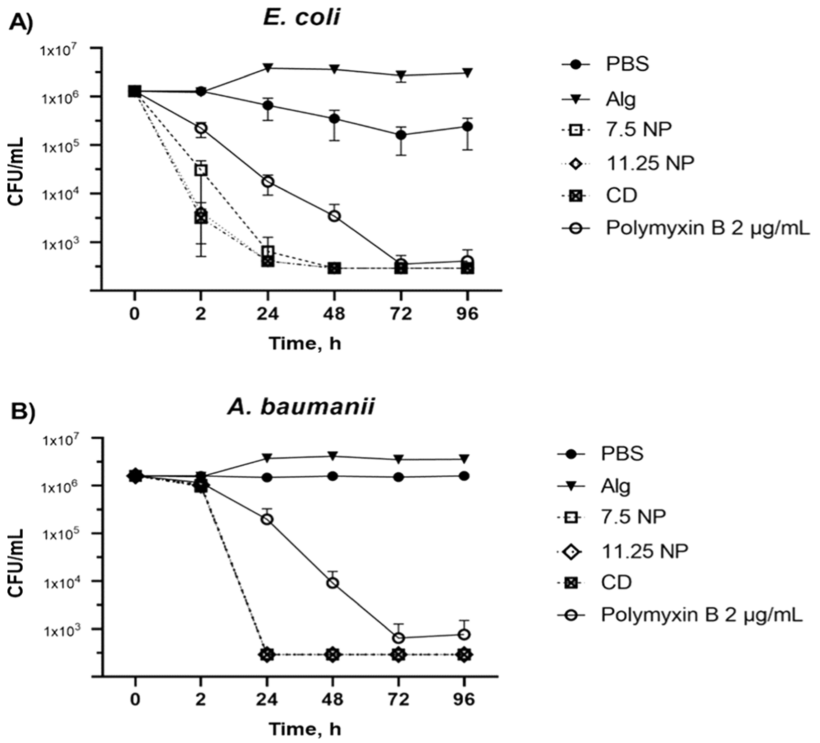

Figure 8. Bactericidal effect of alginate-based aerogels with α-lipoic acid-capped silver nanoparticles (AgNP-ALA). (a) Kinetics of bactericidal effects of aerogels in *E. coli* for 96 h. (b) Kinetics of bactericidal effects of aerogels in *A. baumanii* for 96 h. Strains were incubated with PBS and each of the aerogels to evaluate their bactericidal effect. After 24 h, an evident effect was observed in both strains when aerogels were used. Alg: calcium alginate-PEGMA aerogel. 7.5 NP: calcium alginate-PEGMA aerogel containing 7.5 μg of AgNP-ALAs per aerogel. 11.25 NP: calcium alginate-PEGMA aerogel 11.25 μg AgNP-ALAs per aerogel. CD: commercial silver alginate dressing. Polymyxin B as a positive control (2 μg equivalent to 300 U), and PBS as a negative control or viability control. The bars show the standard deviation of three replicates on different days.

https://doi.org/10.1021/acsomega.3c06114
ACS Omega 2024, 9, 2350−2361

CD had 21.77%, exceeding the 5% established as a high hemocompatibility percentage (Figure 6). The size of AgNPs has been related to cytotoxicity in erythrocytes. Below 50 nm, AgNPs can produce oxidative stress and damage to the membrane, resulting in hemolysis, while high AgNP concentrations such as 20 μg/mL can cause hemolysis of 12−70%.[61] Thus, our aerogels with 60 nm AgNPs are highly hemocompatible regarding hemoglobin release. Topical hemostatic agents such as calcium alginates are used for minor bleeding; besides, they are available as a wound dressing with or without silver.[62] Agents such as calcium alginates are readily available for minor bleeding as a wound dressing. Ion calcium of the alginate is exchanged for sodium in the wound, potentially triggering the coagulation cascade.[4] Alginate dressings are hemostatic and should be used only for wounds with moderate to heavy exudate. Although proved to be effective hemostatic agents, modified alginate can more efficiently control lethal bleeding.[63]

3.4. Viability of *E. coli* and *A. baumanii* in PBS and Antibiotic Susceptibility Assays. Our first goal, when analyzing the antibacterial effect of our aerogels, was to demonstrate that both *A. baumanii* and the reference bacterium *E. coli* could maintain their viability in 1× PBS, a vehicle that is poor in nutrients. Our results demonstrated that *A. baumanii* maintained the bacterial load in 1× PBS after 96 h of incubation without significant changes (Figure 7A). In contrast, the *E. coli* load decreased by 1 log 10 after 48 h of incubation, although it remained viable and culturable (Figure 7A) when it is maintained in 1× PBS. The next step was to investigate the antibiotic concentration required to obtain an inhibition zone diameter comparable to that approved for a reference bacterium (*E. coli*), based on the CLSI (2016).[64] According to the antibiotics evaluated here, *A. baumanii* exposed to 300 U of polymyxin B produces an inhibition zone diameter of 15.8 mm (Figure 7B). Given that the inhibition zone diameter obtained with polymyxin B in the reference strain *E. coli* ATCC 25922 was within the expected range for this bacterium (CLSI, 2016), we chose this antibiotic concentration as antibacterial control to compare it with the antimicrobial effect of our aerogels. Likewise, when observing that the inhibition zones in *E. coli* ATCC 25922 are within the expected range for the other antibiotics, we can validate the method, the antibiotics, and the reference strain (Figure 7B). The disk diffusion assays showed that our aerogels and the commercial dressing (used as a reference) have an antibacterial effect against *E. coli* and *A. baumanii* (Figure 7C).

3.5. Bactericidal Effect of 7.5 NP and 11.25 NP Alginate-Based Aerogels on *E. coli* and *A. baumannii*. Once the experimental conditions were established, that is the culture conditions and antibiotic concentration, our aerogels were analyzed to investigate their antibiotic effect against the MDR *A. baumanii*. After 24 h of incubation with both concentrations of AgNPs-ALA, a reduction of 4Log10 was determined for both strains, *E. coli* and *A. baumannii* (Figure 8). The control polymyxin B concentration for the assays was 2 μg/mL equivalent to 300 U. The number of colony-forming units per mL (cfu/mL) of *E. coli* after 2 h of incubation decreased to the same values as those of CD. After 24 h, the 7.5 NP aerogel reached the same cfu/mL as that of the 11.25 NP and CD. These values were lower than those obtained with polymyxin B (Figure 8A). However, the cfu/mL of the MDR *A. baumanii* strain decreased after 24 h with no differences between 7.5 NP, 11.25 NP, and CD (Figure 8B). Bacterial colonization of wound dressing materials is one of the significant problems in wound healing therapy. The bacteria colonization degree results from the specific microorganism pathogenicity and virulence, in combination with the immunological condition of the patient. In recent years, new approaches have been developed to improve the antimicrobial response, such as antibiotic combinations, bacteriophage therapy, and antimicrobial NP-based formulations. Delivery of AgNPs through aerogels, used for topical administration against MDR bacteria, has been described to improve the AgNPs' antimicrobial activity.[65] This nanostructured material loaded with AgNPs demonstrates biocompatibility with the epithelial human cell line, which also had a remarkable antimicrobial effect on the MDR *A. baumanii* and *E. coli* reference strain as well. These results position the AgNP-ALA biocomposites with the potential to be used in nanotherapeutics to treat MDR microbial infected wounds over open injuries.

4. CONCLUSIONS

In this work, the effects of lipoic acid-capped AgNPs on alginate-based aerogels were studied to investigate their potential biomedical applications. The performance of our aerogels was compared to that of a commercial dressing also made of alginate and containing colloidal silver as the bioactive compound. Based on our results and under the experimental conditions used in this study, the differences in terms of the microstructure and nature of the silver, used as the bioactive agent, between our synthesized aerogels and the commercial dressing used as a reference allowed us to improve several biological properties in our aerogels with respect to the reference commercial material. Our aerogels showed significantly higher antioxidant capacity, in terms of nmol of TEAC/mg aerogel, than the commercial dressing. All our synthesized aerogels showed anti-inflammatory activity, expressed as nmol of IEAC per mg of aerogel, while this property was not present in the commercial dressing material. Finally, our aerogels were highly hemocompatible (less than 1% hemolysis ratio); however, the commercial material showed a 20% hemolysis rate. Regarding antibacterial activity, our alginate-based aerogels containing either 7.5 or 11.25 μg of AgNPs-ALA per aerogel showed equivalent antimicrobial activity against the MDR *A. baumanii* and *E. coli* reference strain, as well, relative to the commercial dressing and polymyxin B. Therefore, our results show the potential of alginate-based aerogels with lipoic acid-capped AgNPs for biomedical applications and makes our aerogels a good choice for further evaluations, such as nanotherapeutics to treat MDR-infected wounds over open injuries.

AUTHOR INFORMATION

Corresponding Authors

Jorge Bravo-Madrigal − *Unidad de Biotecnología Médica y Farmacéutica, Centro de Investigación Asistencia en Tecnología y Diseño de Estado de Jalisco (CIATEJ), C.P. 44270 Guadalajara, Jalisco, Mexico*; Email: jbravo@ciatej.mx

Ana B. Castro-Ceseña − *Departamento de Innovación Biomédica, Centro de Investigación Científica y de Educación Superior de Ensenada, Baja California (CICESE), C.P. 22860 Ensenada, Baja California, Mexico; CONAHCYT-Departamento de Innovación Biomédica, Centro de Investigación Científica y de Educación Superior de Ensenada,*

https://doi.org/10.1021/acsomega.3c06114
ACS Omega 2024, 9, 2350−2361

Baja California (CICESE), C.P. 22860 Ensenada, Baja California, Mexico; orcid.org/0000-0001-8121-7874; Email: acastro@cicese.mx

Authors

Kevin D. Martínez-García − *Departamento de Innovación Biomédica, Centro de Investigación Científica y de Educación Superior de Ensenada, Baja California (CICESE), C.P. 22860 Ensenada, Baja California, Mexico*

Tonatzin Zertuche-Arias − *Departamento de Innovación Biomédica, Centro de Investigación Científica y de Educación Superior de Ensenada, Baja California (CICESE), C.P. 22860 Ensenada, Baja California, Mexico*

Johanna Bernáldez-Sarabia − *Departamento de Innovación Biomédica, Centro de Investigación Científica y de Educación Superior de Ensenada, Baja California (CICESE), C.P. 22860 Ensenada, Baja California, Mexico*

Enrique Iñiguez − *Ciencias de la Tierra and CONAHCYT—Ciencias de la Tierra, Centro de Investigación Científica y de Educación Superior de Ensenada, Baja California (CICESE), C.P. 22860 Ensenada, Baja California, Mexico*

Thomas Kretzchmar − *Ciencias de la Tierra, Centro de Investigación Científica y de Educación Superior de Ensenada, Baja California (CICESE), C.P. 22860 Ensenada, Baja California, Mexico*

Tanya Amanda Camacho-Villegas − *Unidad de Biotecnología Médica y Farmacéutica, Centro de Investigación Asistencia en Tecnología y Diseño de Estado de Jalisco (CIATEJ), C.P. 44270 Guadalajara, Jalisco, Mexico; CONAHCYT-Unidad de Biotecnología Médica y Farmacéutica, Centro de Investigación Asistencia en Tecnología y Diseño del Estado de Jalisco (CIATEJ), C.P. 44270 Guadalajara, Jalisco, Mexico;* orcid.org/0000-0002-0540-0287

Pavel H. Lugo-Fabres − *Unidad de Biotecnología Médica y Farmacéutica, Centro de Investigación Asistencia en Tecnología y Diseño de Estado de Jalisco (CIATEJ), C.P. 44270 Guadalajara, Jalisco, Mexico; CONAHCYT-Unidad de Biotecnología Médica y Farmacéutica, Centro de Investigación Asistencia en Tecnología y Diseño del Estado de Jalisco (CIATEJ), C.P. 44270 Guadalajara, Jalisco, Mexico*

Alexei F. Licea Navarro − *Departamento de Innovación Biomédica, Centro de Investigación Científica y de Educación Superior de Ensenada, Baja California (CICESE), C.P. 22860 Ensenada, Baja California, Mexico;* orcid.org/0000-0003-4022-7405

Complete contact information is available at: https://pubs.acs.org/10.1021/acsomega.3c06114

Author Contributions

Kevin D. Martínez-García performed the conceptualization, methodology, formal analysis, investigation, and writing—original draft. Tonatzin Zertuche-Arias carried out the methodology, formal analysis, investigation, visualization, and writing—review and editing. Johanna Bernáldez-Sarabia executed the methodology, resource procurement, and writing—review and editing. Enrique Iñiguez achieved the methodology and writing—review and editing. Thomas G. Kretzchmar performed the resource procurement and writing—review and editing. Tanya A. Camacho-Villegas achieved the methodology, formal analysis, and writing—review and editing. Pavel H. Lugo-Fabres executed the methodology, formal analysis, and writing—review and editing. Alexei Licea Navarro performed the resource procurement and writing—review and editing. Jorge Bravo-Madrigal completed the methodology, resource procurement, validation, and writing—review and editing. Ana B. Castro-Ceseña performed the conceptualization, methodology, writing—review and editing, visualization, supervision, project administration, and funding acquisition.

Notes

The authors declare no competing financial interest.

■ ACKNOWLEDGMENTS

This work was supported by CICESE (grant no. 685112). We thank Luis Gradilla from Ciencias de la Tierra, CICESE, for his help with SEM imaging and EDX.

■ REFERENCES

(1) Li, J.; Mooney, D. J. *Nat. Rev. Mater.* **2016**, *1*, 16071.

(2) Bashir, S. M.; Ahmed Rather, G.; Patrício, A.; Haq, Z.; Sheikh, A. A.; Shah, M. Z. ul H.; Singh, H.; Khan, A. A.; Imtiyaz, S.; Ahmad, S. B.; Nabi, S.; Rakhshan, R.; Hassan, S.; Fonte, P. *Materials* **2022**, *15*, 6521.

(3) Shahzad, A.; Khan, A.; Afzal, Z.; Umer, M. F.; Khan, J.; Khan, G. M. Formulation development and characterization of cefazolin nanoparticles-loaded cross-linked films of sodium alginate and pectin as wound dressings. *Int. J. Biol. Macromol.* **2019**, *124*, 255−269.

(4) Woo, K. Y.; Sibbald, R. G. Local Wound Care for Malignant and Palliative Wounds. *Palliative Care: Core Skills and Clinical Competencies, Expert Consult Online and Print* **2010**, *23*, 417−428.

(5) Chetter, I. C.; Oswald, A. V.; Mcginnis, E.; Stubbs, N.; Arundel, C.; Buckley, H.; Bell, K.; Dumville, J. C.; Cullum, N. A.; Soares, M. O.; Saramago, P. Patients with surgical wounds healing by secondary intention: A prospective, cohort study. *Int. J. Nurs. Stud.* **2019**, *89*, 62−71.

(6) Probst, S.; Arber, A.; Faithfull, S. Malignant fungating wounds: A survey of nurses' clinical practice in Switzerland. *Eur. J. Oncol. Nurs.* **2009**, *13*, 295−298.

(7) Ubbink, D. T.; Vermeulen, H.; Goossens, A.; Kelner, R. B.; Schreuder, S. M.; Lubbers, M. J. Occlusive vs Gauze Dressings for Local Wound Care in Surgical Patients: A Randomized Clinical Trial. *Arch. Surg.* **2008**, *143*, 950−955.

(8) Vermeulen, H.; van Hattem, J. M.; Storm-Versloot, M. N.; Ubbink, D. T.; Westerbos, S. J. Topical silver for treating infected wounds. *Cochrane Database Syst. Rev.* **2007**, No. 1, No. CD005486.

(9) Sikora, A.; Zahra, F. *Nosocomial Infections*; StatPearls Publishing, 2022.

(10) Shariati, A.; Moradabadi, A.; Ghaznavi-Rad, E.; Dadmanesh, M.; Komijani, M.; Nojoomi, F. *Ann. Clin. Microbiol. Antimicrob.* **2021**, *20*, 40.

(11) Zurawski, D. v.; Banerjee, J.; Alamneh, Y. A.; Shearer, J. P.; Demons, S. T. Skin and Soft Tissue Models for Acinetobacter baumannii Infection. *Methods Mol. Biol.* **2019**, *1946*, 271−287.

(12) Salunke, G. R.; Ghosh, S.; Santosh Kumar, R. J.; Khade, S.; Vashisth, P.; Kale, T.; Chopade, S.; Pruthi, V.; Kundu, G.; Bellare, J. R.; Chopade, B. A. Rapid efficient synthesis and characterization of silver, gold, and bimetallic nanoparticles from the medicinal plant Plumbago zeylanica and their application in biofilm control. *Int. J. Nanomed.* **2014**, *9*, 2635−2653.

(13) Hassan, A.; Ikram, A.; Raza, A.; Saeed, S.; Zafar Paracha, R.; Younas, Z.; Khadim, M. T. Therapeutic Potential of Novel Mastoparan-Chitosan Nanoconstructs Against Clinical MDR Acinetobacter baumannii: In silico, in vitro and in vivo Studies. *Int. J. Nanomed.* **2021**, *16*, 3755−3773.

(14) Puca, V.; Marulli, R. Z.; Grande, R.; Vitale, I.; Niro, A.; Molinaro, G.; Prezioso, S.; Muraro, R.; di Giovanni, P. *Antibiotics* **2021**, *10*, 1162.

(15) Langemo, D. K.; Brown, G. *Adv. Skin Wound Care* **2006**, *19*, 206−211.

(16) Ferris, F. D.; Abdullah, A.; Khateib, A. L.; Fromantin, I.; Hoplamazian, L.; Hurd, T.; Krasner, D. L.; Maida, V.; Price, P.; Ps, A. F. B. S.; Rich-Vanderbij, L. *J. Palliat. Med.* **2007**, *10*, 37−40.
(17) Beers, E. H. Palliative Wound Care. *Surg. Clin. N. A.* **2019**, *99*, 899−919.
(18) Ignatova, M.; Rashkov, I.; Manolova, N. Drug-loaded electrospun materials in wound-dressing applications and in local cancer treatment. *Expert Opin. Drug Deliv.* **2013**, *10*, 469−483.
(19) Ahmad Raus, R.; Wan Nawawi, W. M. F.; Nasaruddin, R. R. Alginate and alginate composites for biomedical applications. *Asian J. Pharm. Sci.* **2021**, *16*, 280−306.
(20) Broussard, K. C.; Powers, J. G. Wound Dressings: Selecting the Most Appropriate Type. *Am. J. Clin. Dermatol.* **2013**, *14*, 449−459.
(21) Duckworth, P. F.; Maddocks, S. E.; Rahatekar, S. S.; Barbour, M. E. *J. Mater. Sci. Mater. Med.* **2020**, *31*, 33.
(22) Percival, S. L.; Slone, W.; Linton, S.; Okel, T.; Corum, L.; Thomas, J. G. The antimicrobial efficacy of a silver alginate dressing against a broad spectrum of clinically relevant wound isolates. *Int. Wound J.* **2011**, *8*, 237−243.
(23) Bonomo, P.; Desideri, I.; Loi, M.; Ciccone, L. P.; lo Russo, M.; Becherini, C.; Greto, D.; Simontacchi, G.; Pimpinelli, N.; Livi, L. Management of severe bio-radiation dermatitis induced by radiotherapy and cetuximab in patients with head and neck cancer: emphasizing the role of calcium alginate dressings. *Support. Care Cancer* **2019**, *27*, 2957−2967.
(24) Asadi, L.; Mokhtari, J.; Abbasi, M. *J. Mater. Sci. Mater. Med.* **2021**, *32*, 7.
(25) Cotton, G. C.; Gee, C.; Jude, A.; Duncan, W. J.; Abdelmoneim, D.; Coates, D. E. Efficacy and safety of alpha lipoic acid-capped silver nanoparticles for oral applications. *RSC Adv.* **2019**, *9*, 6973−6985.
(26) Ichimura, T.; et al. *Sci. Rep.* **2021**, *11*, 16539.
(27) Stagnaro, P.; Schizzi, I.; Utzeri, R.; Marsano, E.; Castellano, M. Alginate-polymethacrylate hybrid hydrogels for potential osteochondral tissue regeneration. *Carbohydr. Polym.* **2018**, *185*, 56−62.
(28) Saha, N. R.; Roy, I.; Sarkar, G.; Bhattacharyya, A.; Das, R.; Rana, D.; Banerjee, R.; Paul, A. K.; Mishra, R.; Chattopadhyay, D. Development of active packaging material based on cellulose acetate butyrate/polyethylene glycol/aryl ammonium cation modified clay. *Carbohydr. Polym.* **2018**, *187*, 8−18.
(29) Rubio-Elizalde, I.; Bernáldez-Sarabia, J.; Moreno-Ulloa, A.; Vilanova, C.; Juárez, P.; Licea-Navarro, A.; Castro-Ceseña, A. B. Scaffolds based on alginate-PEG methyl ether methacrylate-Moringa oleifera-Aloe vera for wound healing applications. *Carbohydr. Polym.* **2019**, *206*, 455−467.
(30) Li, Q.; Gong, S.; Yao, W.; Yu, Y.; Liu, C.; Wang, R.; Pan, H.; Wei, M. PEG-interpenetrated genipin-crosslinked dual-sensitive hydrogel/nanostructured lipid carrier compound formulation for topical drug administration. *Artif. Cells, Nanomed., Biotechnol.* **2021**, *49*, 345−353.
(31) Wang, T.; Li, Y.; Liu, Y.; Xu, Z.; Wen, M.; Zhang, L.; Xue, Y.; Shang, L. Highly biocompatible Ag nanocluster-reinforced wound dressing with long-term and synergistic bactericidal activity. *J. Colloid Interface Sci.* **2023**, *633*, 851−865.
(32) Sharma, J. N.; Al-Omran, A.; Parvathy, S. S. Role of nitric oxide in inflammatory diseases. *Inflammopharmacology* **2007**, *15*, 252−259.
(33) Zmora, S.; Glicklis, R.; Cohen, S. Tailoring the pore architecture in 3-D alginate scaffolds by controlling the freezing regime during fabrication. *Biomaterials* **2002**, *23*, 4087−4094.
(34) Haroon, M.; Zaidi, A.; Ahmed, B.; Rizvi, A.; Khan, M. S.; Musarrat, J. Effective Inhibition of Phytopathogenic Microbes by Eco-Friendly Leaf Extract Mediated Silver Nanoparticles (AgNPs). *Indian J. Microbiol.* **2019**, *59*, 273−287.
(35) Re, R.; Pellegrini, N.; Proteggente, A.; Pannala, A.; Yang, M.; Rice-Evans, C. Antioxidant activity applying an improved ABTS radical cation decolorization assay. *Free Radical Biol. Med.* **1999**, *26*, 1231−1237.
(36) Gomez-Aparicio, L. S.; Bernáldez-Sarabia, J.; Camacho-Villegas, T. A.; Lugo-Fabres, P. H.; Díaz-Martínez, N. E.; Padilla-Camberos, E.; Licea-Navarro, A.; Castro-Ceseña, A. B. Improvement of the wound healing properties of hydrogels with N-acetylcysteine through their modification with methacrylate-containing polymers. *Biomater. Sci.* **2021**, *9*, 726−744.
(37) Pardau, M. D.; Pereira, A. S. P.; Apostolides, Z.; Serem, J. C.; Bester, M. J. Antioxidant and anti-inflammatory properties of Ilex guayusatea preparations: a comparison to Camellia sinensisteas. *Food Funct.* **2017**, *8*, 4601−4610.
(38) Ooi, C. H.; Ling, Y. P.; Abdullah, W. Z.; Mustafa, A. Z.; Pung, S. Y.; Yeoh, F. Y. *J. Mater. Sci. Mater. Med.* **2019**, *30*, 44.
(39) Patel, J. B.; Cockerill, P. A., III; Bradford, F. R.; Eliopoulos, G. M.; Hindler, J. A.; Jenkins, S. G.; Lewis, J. S., II; Limbago, B.; Miller, L. A.; Nicolau, D. P.; Powell, M.; Swenson, J. M.; Traczewski, M. M.; Turnidge, J. D.; Weinstein, M. P.; Zimmer, B. L.; *M07-A9. Methods for Dilution Antimicrobial Susceptibility Tests for Bacteria That Grow Aerobically*; Clinical and Laboratory Standards Institute, 2015; Vol. *32*.
(40) Flemming, R. G.; Murphy, C. J.; Abrams, G. A.; Goodman, S. L.; Nealey, P. F. Effects of synthetic micro- and nano-structured surfaces on cell behavior. *Biomaterials* **1999**, *20*, 573−588.
(41) Hollister, S. J. Porous scaffold design for tissue engineering. *Nat. Mater.* **2005**, *4*, 518−524.
(42) Yang, J.; Shi, G.; Bei, J.; Wang, S.; Cao, Y.; Shang, Q.; Yang, G.; Wang, W. Fabrication and surface modification of macroporous poly(L-lactic acid) and poly(L-lactic-co-glycolic acid) (70/30) cell scaffolds for human skin fibroblast cell culture. *J. Biomed. Mater. Res.* **2002**, *62*, 438−446.
(43) Madden, L. R.; Mortisen, D. J.; Sussman, E. M.; Dupras, S. K.; Fugate, J. A.; Cuy, J. L.; Hauch, K. D.; Laflamme, M. A.; Murry, C. E.; Ratner, B. D. Proangiogenic scaffolds as functional templates for cardiac tissue engineering. *Proc. Natl. Acad. Sci. U.S.A.* **2010**, *107*, 15211−15216.
(44) Artel, A.; Mehdizadeh, H.; Chiu, Y. C.; Brey, E. M.; Cinar, A. An Agent-Based Model for the Investigation of Neovascularization Within Porous Scaffolds. *Tissue Eng. Part A* **2011**, *17*, 2133−2141.
(45) Gao, C.; Pollet, E.; Avérous, L. Innovative plasticized alginate obtained by thermo-mechanical mixing: Effect of different biobased polyols systems. *Carbohydr. Polym.* **2017**, *157*, 669−676.
(46) Porter, G. C.; Schwass, D. R.; Tompkins, G. R.; Bobbala, S. K. R.; Medlicott, N. J.; Meledandri, C. J. AgNP/Alginate Nanocomposite hydrogel for antimicrobial and antibiofilm applications. *Carbohydr. Polym.* **2021**, *251*, 117017.
(47) Papageorgiou, S. K.; Kouvelos, E. P.; Favvas, E. P.; Sapalidis, A. A.; Romanos, G. E.; Katsaros, F. K. Metal−carboxylate interactions in metal−alginate complexes studied with FTIR spectroscopy. *Carbohydr. Res.* **2010**, *345*, 469−473.
(48) Cui, J.; Shao, Y.; Zhang, H.; Zhang, H.; Zhu, J. Development of a novel silver ions-nanosilver complementary composite as antimicrobial additive for powder coating. *Chem. Eng. J.* **2021**, *420*, 127633.
(49) Jyoti, K.; Baunthiyal, M.; Singh, A. Characterization of silver nanoparticles synthesized using Urtica dioica Linn. leaves and their synergistic effects with antibiotics. *J. Radiat. Res. Appl. Sci.* **2016**, *9*, 217−227.
(50) Cai, K.; Bossert, J.; Jandt, K. D. *Colloids Surf., B* **2006**, *49*, 136−144.
(51) Galli, C.; Collaud Coen, M.; Hauert, R.; Katanaev, V. L.; Gröning, P.; Schlapbach, L. Creation of nanostructures to study the topographical dependency of protein adsorption. *Colloids Surf., B* **2002**, *26*, 255−267.
(52) Ďuračková, Z. Some Current Insights into Oxidative Stress. *Physiol. Res.* **2010**, *59*, 459−469.
(53) Petersen Shay, K.; Moreau, R. F.; Smith, E. J.; Hagen, T. M. *IUBMB Life* **2008**, *60*, 362−367.
(54) Goraca, A.; Huk-Kolega, H.; Piechota, A.; Kleniewska, P.; Ciejka, E.; Skibska, B. Lipoic acid − biological activity and therapeutic potential. *Pharmacol. Rep.* **2011**, *63*, 849−858.
(55) Anwar, N.; Wahid, J.; Uddin, J.; Khan, A.; Shah, M.; Shah, S. A.; Subhan, F.; Khan, M. A.; Ali, K.; Rauf, M.; Arif, M. Phytosynthesis of poly (ethylene glycol) methacrylate-hybridized gold nanoparticles

https://doi.org/10.1021/acsomega.3c06114
ACS Omega 2024, 9, 2350−2361

from C. tuberculata: their structural characterization and potential for in vitro growth in banana. *In Vitro Cell. Dev. Biol. Plant* **2021**, *57*, 248−260.
(56) Anwar, N.; Khan, A.; Shah, M.; Walsh, J. J.; Saleem, S.; Anwar, Z.; Aslam, S.; Irshad, M. Hybridization of green synthesized silver nanoparticles with poly(ethylene glycol) methacrylate and their biomedical applications. *PeerJ* **2022**, *10*, No. e12540.
(57) Miller, N. J.; Rice-Evans, C.; Davies, M. J.; Gopinathan, V.; Milner, A. A Novel Method for Measuring Antioxidant Capacity and its Application to Monitoring the Antioxidant Status in Premature Neonates. *Clin. Sci.* **1993**, *84*, 407−412.
(58) Chen, L.; Deng, H.; Cui, H.; Fang, J.; Zuo, Z.; Deng, J.; Li, Y.; Wang, X.; Zhao, L. Inflammatory responses and inflammation-associated diseases in organs. *Oncotarget* **2018**, *9*, 7204−7218.
(59) Ridnour, L. A.; Thomas, D. D.; Switzer, C.; Flores-Santana, W.; Isenberg, J. S.; Ambs, S.; Roberts, D. D.; Wink, D. A. Molecular mechanisms for discrete nitric oxide levels in cancer. *Nitric Oxide* **2008**, *19*, 73−76.
(60) Ackland, G. L.; Gutierrez Del Arroyo, A.; Yao, S. T.; Stephens, R. C.; Dyson, A.; Klein, N. J.; Singer, M.; Gourine, A. v. Low-molecular-weight polyethylene glycol improves survival in experimental sepsis*. *Crit. Care Med.* **2010**, *38*, 629−636.
(61) Chen, L. Q.; Fang, L.; Ling, J.; Ding, C. Z.; Kang, B.; Huang, C. Z. Nanotoxicity of Silver Nanoparticles to Red Blood Cells: Size Dependent Adsorption, Uptake, and Hemolytic Activity. *Chem. Res. Toxicol.* **2015**, *28*, 501−509.
(62) Alexander, S. Malignant fungating wounds: managing pain, bleeding and psychosocial issues. *J. Wound Care* **2009**, *18*, 418−425.
(63) Dowling, M. B.; Chaturvedi, A.; MacIntire, I. C.; Javvaji, V.; Gustin, J.; Raghavan, S. R.; Scalea, T. M.; Narayan, M. Determination of efficacy of a novel alginate dressing in a lethal arterial injury model in swine. *Injury* **2016**, *47*, 2105−2109.
(64) Weinstein, M. P.; Lewis, J. S., II; Bobenchik, A. M.; Campeau, S.; Cullen, S. K.; Galas, M. F.; Gold, H.; Humphries, R. M., Jr.; Kirn, T. J.; Limbago, B.; Mathers, A. J.; Mazzulli, T.; Satlin, M.; Schuetz, A. N.; Simner, P. J.; Tamma, P. D. *M100-S26. Performance Standards for Antimicrobial Susceptibility Testing*, 26th ed.; Clinical and Laboratory Standards Institute: Wayne, PA, 2016.
(65) Mekkawy, A. I.; El-Mokhtar, M. A.; Nafady, N. A.; Yousef, N.; Hamad, M.; El-Shanawany, S. M.; Ibrahim, E. H.; Elsabahy, M. In vitro and in vivo evaluation of biologically synthesized silver nanoparticles for topical applications: effect of surface coating and loading into hydrogels. *Int. J. Nanomed.* **2017**, *12*, 759−777.

https://doi.org/10.1021/acsomega.3c06114
ACS Omega 2024, 9, 2350−2361